Marine Vehicles' Line Following Controller Tuning through Self-Oscillation Experiments

Nikola Miskovic and Zoran Vukic
Faculty of Electrical Engineering and Computing
University of Zagreb, Unska 3, Zagreb, Croatia
E-mail: {nikola.miskovic, zoran.vukic}@fer.hr

Marco Bibuli, Massimo Caccia and Gabriele Bruzzone
Consiglio Nazionale delle Ricerche, ISSIA
Via de Marini 6, Genova, Italy
E-mail: {marco, max, gabry}@ge.issia.cnr.it

***Abstract*—This paper demonstrates the use of self-oscillation identification experiments for tuning line following controllers for marine vehicles. Two approaches are described: first, when the controller output is yaw rate and second when controller output is reference heading. In the first case, low level controller is yaw rate while in the second it is heading controller. The identification by use of self-oscillations (IS-O) has been applied to identify the steering equation (for the case of the first controller) and it was used to identify the heading closed loop (for the case of the second controller). The second controller has been tested on different inner loop structures in order to prove the functionality of the method. The IS-O method has been chosen because of its simplicity and applicability in the field (effects of external disturbances are minimized). The methodology was applied to autonomous catamaran Charlie. The results are presented in the paper and demonstrate that the proposed method for identification as well as the developed algorithms give satisfactory performance. All algorithms and results presented here are a result of a joint work of researchers at the Consiglio Nazionale delle Ricerche, Genova and the University of Zagreb.**

Fig. 1. Unmanned surface vehicle Charlie.

I. Introduction

Control of unmanned marine vehicles is commonly divided in three levels. The principle level of control is motion control and it usually implies the control of yaw and surge velocities. Mid control level, or guidance control, has the task to generate reference signals for the low level controllers. This level implies heading control and trajectory and/or path following. Trajectory following implies following a time-parameterized curve, while path following implies following a planar path without temporal constraints. Finally, the upper level of control includes mission planning. This paper will address the problem of path following - the main objective is to have the vessel converge to a desired path and follow it regardless of the external disturbances (sea currents, wind, etc.). The first step to designing any type of controller is identification of system dynamics. Usually, identification of marine vehicles' mathematical model is performed in open loop where a great number of experiments have to be performed. Identification procedure for autonomous catamaran Charlie is reported in [1], while similar techniques used on underwater vehicles are reported in [2], [3], [4]. All these experiments are based on finding the vehicle's drag (from steady-state experiments) and inertia (from zig-zag manoeuvres or open-loop transient characteristic). The greatest advantage of these identification techniques is that the model parameters can be determined with great precision given enough experimental data. On the other hand, the disadvantages are the effects of the omnipresent external disturbances on the identified parameters, and the fact that the procedure itself is time-consuming.

The identification method which has been proposed here is based on self-oscillations, [5]. The motivation for introducing this method comes from the fact reported in [6] that due to the closed loop procedure the influence of external disturbances is minimized. In addition to that, the algorithm itself is very time conservative and is easily automated. On the other hand, in order to use this method, exact mathematical model of the identified process has to be known. Also, due to assumptions on the higher harmonics, the identified parameters can slightly differ from the real values.

The paper is organized as follows. This section is followed by description of Charlie catamaran, gives line following equations and a short introduction to self-oscillations. Section 2 describes the application of self-oscillation identification method to marine vehicles. In Section 3, two approaches to designing line following controllers are presented. Experimental results are given in Section 4 and the paper is concluded with Section 5.

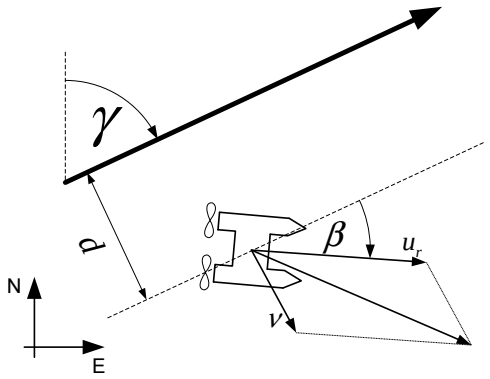

Fig. 2. Line following.

A. Charlie USV

The Charlie USV (see Fig. 1) is a small catamaran-like shape prototype vehicle originally developed by the CNR-ISSIA for the sampling of the sea surface microlayer and immediate subsurface for the study of the sea-air interaction, [7]. Charlie is 2.40 m long, 1.70 m wide and weighs about 300 kg in air. The propulsion system of the vehicle is composed of a couple of DC motors (300 W @ 48 V). The vehicle is equipped with a rudder-based steering system, where two rigidly connected rudders, positioned behind the thrusters, are actuated by a brushless DC motor. The navigation instrumentation set is constituted of a GPS Ashtech GG24C integrated with compass KVH Azimuth Gyrotrac able to compute the True North. The on-board real-time control system, developed in C++, is based on GNU/Linux and run on a Single Board Computer (SBC) which supports serial and Ethernet communications and PC-104 modules for digital and analog I/O. The steering equation of Charlie can be described with (1) where r is yaw rate, ψ is heading, τ_N commanded yaw torque, and parameters to be identified are yaw inertia I_r, and drag $k_{r|r|}$ (see [1] for details on model parameters).

$$\begin{aligned} I_r\dot{r} &= -\tilde{k}_{r|r|}r|r| + \tau_N \\ \dot{\psi} &= r \end{aligned} \tag{1}$$

For Charlie ASV, the yaw torque control is described with $\tau_N = n^2\delta$ where δ is the rudder angle and n is propeller revolution rate.

B. Line Following Equations

The line following approach is shown in Fig. 2. The aim is to steer the vehicle moving at surge speed u_r in such a way that its path converges to the desired line. If γ is orientation of the line that should be followed, a new parameter $\beta = \psi - \gamma$ (vehicle's orientation relative to the line) is defined. Having this in mind, the line following equations (2) - (5) can be written, where ν is drift due to external disturbances which is perpendicular to the direction of the desired path.

$$\dot{r} = -\frac{k_{r|r|}}{I_r}r|r| + \frac{1}{I_r}\tau_N \tag{2}$$

$$\dot{\psi} = r \tag{3}$$

$$\dot{\beta} = r \tag{4}$$

$$\dot{d} = u_r \sin\beta + \nu \tag{5}$$

The nonlinearities of the line-following model appear in (2) and (5). The first one can be eliminated by introducing a low level yaw rate or heading feedback. The second nonlinear equation can be linearized if angle β is assumed to be small. In that case, (5) can be rewritten as $\dot{d} = u_r\beta + \nu$.

C. Identification by Use of Self-Oscillations (IS-O)

The idea of using self-oscillations to determine system parameters was introduced in [8]. Since then, the method has been applied in process industry for tuning controllers. First application of the method in marine control was introduced on underwater vehicles and is reported in [9] and [10]. Since then, it has also been applied for heading controller tuning of marine surface vehicles, [11]. The self-oscillation experiment is done in closed loop which consists of a nonlinear element, the process and a unity feedback. The method is based upon forcing the system into self-oscillations - the magnitude X_m and frequency ω of the obtained self-oscillations can be used to determine the process' parameters. The link between the space of process' parameters and the space of magnitudes and frequencies of self-oscillations is the Goldfarb principle given with

$$G_P(j\omega) = -\frac{1}{G_N(X_m)} = -\frac{1}{P_N(X_m) + jQ_N(X_m)} \tag{6}$$

where $G_N(X_m) = P_N(X_m) + jQ_N(X_m)$ is the describing function of the nonlinear element and $G_P(j\omega)$ is the process frequency characteristic, [5]. It should be stressed that the nonlinearity mostly used in the closed loop is a relay with hysteresis, but need not necessarily be. However, there are some advantages which made this element most commonly used in practice: *a)* every system whose Nyquist characteristic passes through the II quadrant can be caused to oscillate; *b)* it is insensitive to noise and *c)* it is easily implementable, [5]. In the case of relay with hysteresis, the describing function parameters are $P(X_m) = \frac{4C}{\pi X_m}\sqrt{1 - \left(\frac{x_a}{X_m}\right)^2}$ and $Q(X_m) = -\frac{4C}{\pi X_m^2}x_a$, where C is relay output and x_a is hysteresis width. Detailed derivation of the general algorithm for determining parameters of an LTI process of n-th order can be found in [12]. The same paper includes modifications for astatic systems and systems with delays. In the following subsections only final results of the algorithm for linear systems and methodology for using the proposed method on nonlinear systems are given.

II. IS-O Applied to Marine Vehicles

A. Identifying Steering Equation

The steering equation of marine vehicles can be described using (1). The proposed identification by use of

TABLE I
HEADING CLOSED LOOP TRANSFER FUNCTIONS DEPENDING ON THE CONTROL ALGORITHM ($e = \psi_{ref} - \psi$)

Name	Algorithm	$\frac{\psi}{\psi_{ref}}$
P	$K_P\psi$	$\frac{KK_P}{Ts^2+s+KK_P}$
PD	$K_P\psi + K_D\dot{e}$	$\frac{KK_R+KK_Ds}{Ts^2+(1+KK_D)s+KK_R}$
P-D	$K_Pe + K_D\dot{\psi}$	$\frac{KK_P}{Ts^2+KK_Ds+KK_P}$
PI	$K_Pe + K_I\int e$	$\frac{KK_I+KK_Ps}{Ts^3+s^2+KK_Ps+KK_I}$
I-P	$-K_P\psi + K_I\int e$	$\frac{KK_I}{Ts^3+s^2+KK_Ps+KK_I}$
PID	$K_Pe + K_D\dot{e} + K_I\int e$	$\frac{KK_Ds^2+KK_Ps+KK_I}{Ts^3+(1+KK_D)s^2+KK_Ps+KK_I}$
PI-D	$K_Pe + K_I\int e - K_D\dot{\psi}$	$\frac{KK_Ps+KK_I}{Ts^3+(1+KK_D)s^2+KK_Ps+KK_I}$
I-PD	$K_I\int e - K_P\psi - K_D\dot{\psi}$	$\frac{KK_I}{Ts^3+(1+KK_D)s^2+KK_Ps+KK_I}$

self-oscillations can also be used on nonlinear systems. If the system is in oscillatory regime (due to the presence of the nonlinear element) and under the assumption that the oscillations are symmetric, heading and its derivations can be written as $\psi = X_m\sin(\omega t)$, $\dot{\psi} = X_m j\omega\sin(\omega t)$ and $\ddot{y} = -X_m\omega^2\sin(\omega t)$. Unity feedback implies that $\tau_N = -G_N(X_m)\psi$. Combining these equations with (1), a nonlinear trigonometric equation is obtained. By developing the nonlinear term into a Fourier series where only the first harmonic is retained, $\cos(\omega t)\,|\cos(\omega t)| \approx j\frac{8}{3\pi}\sin(\omega t)$, (7) and (8) can be derived.

$$I_r = \frac{P_N}{\omega^2} \tag{7}$$

$$k_{r|r|} = -\frac{3\pi}{8}\frac{Q_N}{X_m\omega^2} \tag{8}$$

B. Identifying Heading Closed Loop

Heading controllers can have different structures. Naturally, heading closed loops depend on these structures. For heading control it is rather important to have smooth control signals, especially if actuators cannot bear abrupt changes (e.g. rudders) which occur during step reference changes. This is why "-" controllers are often used, e.g. I-PD controller implies that the control difference is taken through the integration channel, while proportional and derivative channel are connected directly to heading, [13]. This can be quite convenient, especially if we note that the derivation channel connected to the heading signal is in fact the yaw rate measurement which is almost always available. Table I shows heading closed loop transfer functions for numerous control algorithms under the assumption that the steering equation is described with a Nomoto model. This assumption does not limit the application of the proposed procedure since the control algorithm can be modified in such a way that the nonlinearity inherent to the steering equation can be compensated for, e.g. as described in [14]. All algorithms, except for classic PID, have at most three poles and one finite zero. We will exclude the classic PID algorithm due to the fact that leading the control difference directly through the derivation channel can seriously damage the actuator. In practice, PI-D controller is used instead. Having this in mind, the general self-oscillation algorithm which has been introduced in [12] will be used to identify a third order transfer function with one finite zero. The general algorithm formulation is omitted due to limited space.

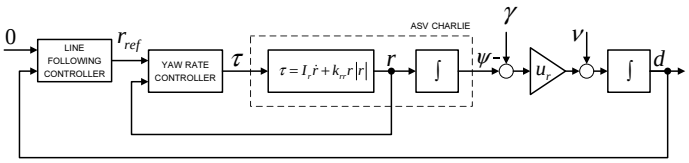

Fig. 3. Line following control structure - Method 1

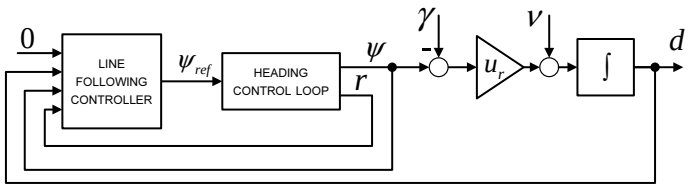

Fig. 4. Line following control structure - Method 2

Let us suppose that heading closed loop transfer function can be written as in (9).

$$\frac{\psi}{\psi_{ref}} = \frac{b_{1\psi}s + 1}{a_{3\psi}s^3 + a_{2\psi}s^2 + a_{1\psi}s + 1} \tag{9}$$

With an assumption that heading closed loop gain is 1, i.e. $b_0 = 1$, and using the procedure presented in [12] with $n = 3$ and $m = 1$, after redundant measurements are omitted, algorithm (10) can be applied.

$$\begin{bmatrix} 0 & -\omega_1^2 & 0 & -\omega_1 Q_1 \\ 0 & -\omega_2^2 & 0 & -\omega_2 Q_2 \\ \omega_1 & 0 & \omega_1^3 & \omega_1 P_1 \\ \omega_2 & 0 & \omega_2^3 & \omega_2 P_2 \end{bmatrix} \begin{bmatrix} a_{1\psi} \\ a_{2\psi} \\ a_{3\psi} \\ b_{1\psi} \end{bmatrix} = \begin{bmatrix} -1 - P_1 \\ -1 - P_2 \\ -Q_1 \\ -Q_2 \end{bmatrix} \tag{10}$$

In (10), $\omega = [\ \omega_1 \ \cdots \ \omega_\varepsilon\ ]^T$, $\mathbf{P} = [\ P_1 \ \cdots \ P_\varepsilon\ ]^T$ and $\mathbf{Q} = [\ Q_1 \ \cdots \ Q_\varepsilon\ ]^T$ are vectors of measurements where elements P_i and Q_i are real and imaginary parts of the nonlinear element, respectively, and ω_i frequency of the self-oscillations obtained in the i-th experiment. The unknown parameters are easily obtained by solving the matrix equation.

III. LINE-FOLLOWING CONTROLLER FOR CHARLIE ASV

Line following controllers can be implemented using two procedures. First is to generate reference yaw rate, which implies that the inner closed loop is yaw rate based as shown in Fig. 3 (Method 1). The second approach is to generate referent heading as output from the line following controller (Method 2). This implies that there exists and inner heading-based closed loop as shown in Fig. 4. If inner closed loop controller can be tuned, than Method 1 is advised because of its simplicity. If heading controller already exists and its structure or parameters cannot be changed, Method 2 is advised because line following controller is tuned without changing the dynamics of the inner control loop. Design procedure for both methods is described in the following sections.

A. Controller Design - Method 1

This method assumes that the low level controller is a yaw rate controller, i.e. the line following controller gives referent yaw rate r_{ref}, as output. First we give the yaw rate closed loop transfer function design, and than the line following controller design is presented.

1) Yaw rate controller: The yaw rate controller is a P-D controller modified to compensate the process' nonlinearity, and it is given with (11).

$$\tau_N = K_{Ir} \int_0^t (r_{ref} - r)\, dt - K_{Pr} r + \tilde{k}_{rr} r\, |r| \tag{11}$$

The inner closed loop transfer function is

$$\frac{r}{r_{ref}} = \frac{1}{\underbrace{\frac{\tilde{I}_r}{K_{Ir}}}_{a_{2r}} s^2 + \underbrace{\frac{K_{Pr}}{K_{Ir}}}_{a_{1r}} s + 1}$$

where a_{2r} and a_{1r} are the desired closed loop transfer function parameters. The controller parameters are then given with (12).

$$K_{Pr} = \frac{a_{1r}}{a_{2r}} \qquad K_{Ir} = \frac{\tilde{I}_r}{a_{2r}} \tag{12}$$

2) Line following controller: According to Fig. 3, open loop transfer function is given with $\frac{d}{r_{ref}} = \frac{u_r}{s^2}\frac{r}{r_{ref}}$, the line following controller is given with

$$r_{ref} = K_{Pd}\,(d_{ref} - d) + K_{Dd}\frac{d}{dt}\,(d_{ref} - d) \tag{13}$$

which yields the closed-loop transfer function given with (14) where a_{4d}, a_{3d}, a_{2d} and a_{1d} are desired line following closed loop transfer function parameters.

$$\frac{d}{d_{ref}} = \frac{1 + \frac{K_{Dd}}{K_{Pd}} s}{\underbrace{\frac{a_{2r}}{u_r K_{Pd}}}_{a_{4d}} s^4 + \underbrace{\frac{a_{1r}}{u_r K_{Pd}}}_{a_{3d}} s^3 + \underbrace{\frac{1}{u_r K_{Pd}}}_{a_{2d}} s^2 + \underbrace{\frac{K_{Dd}}{K_{Pd}}}_{a_{1d}} s + 1} \tag{14}$$

Combining (12) and (14), the line following controller parameters can be calculated using (15).

$$\begin{array}{ll} K_{Ir} = \frac{a_{2d}}{a_{4d}}\tilde{I}_r & K_{Pr} = \frac{a_{3d}}{a_{4d}}\tilde{I}_r \\ K_{Pd} = \frac{1}{u_r a_{2d}} & K_{Dd} = \frac{a_{1d}}{u_r a_{2d}} \end{array} \tag{15}$$

Now it is clear that by setting the desired line following closed loop dynamics, the inner closed loop parameters are set automatically.

3) Algorithm: The algorithm for designing line following controllers according to Method 1 can be summarized as follows.

I Perform one self-oscillation experiment on open loop steering system (1) and determine magnitude X_m and frequency ω of self-oscillations.
II Calculate $\tilde{I}_r$ and $\tilde{k}_{r|r|}$ using (7) and (8).
III Define desired line-following closed loop dynamics (a_{4d}, a_{3d}, a_{2d} and $a_{1\psi}$).
IV Calculate yaw rate and line-following controller parameters using (15) and identified $\tilde{I}_r$.
V Implement yaw rate (11) and line following (13) controllers.

B. Controller Design - Method 2

As it was already mentioned, in this case the only tunable controller is the line following controller which gives referent heading ψ_{ref}, as output. It is shown in II-B that the closed loop heading control can be approximated with 3 poles and a zero giving the transfer function in a form (16).

$$\frac{\psi}{\psi_{ref}} = \frac{b_{1\psi} s + 1}{a_{3\psi} s^3 + a_{2\psi} s^2 + a_{1\psi} s + 1} \tag{16}$$

The parameters in (16) are not known so two self-oscillation experiments have to be carried out as described in II-B. For the purpose of controller tuning, transfer function (16) is simplified using the Algorithm for simplification of heading closed loop transfer function and results in a transfer function with two poles and one finite zero.

1) Algorithm for simplification of heading closed loop transfer function:

I Calculate additional parameters Q, R, D, S and T.
$$Q = \frac{1}{9a_{3\psi}^2}(3a_{1\psi}a_{3\psi} - a_{2\psi}^2)$$
$$R = \frac{1}{54a_{3\psi}^3}(9a_{3\psi}a_{2\psi}a_{1\psi} - 27a_{3\psi}^2 - 2a_{2\psi}^3)$$
$$D = Q^3 + R^2$$
$$S = \sqrt[3]{R + \sqrt{D}}$$
$$T = \sqrt[3]{R - \sqrt{D}}$$
II Find the real pole $p = -\frac{1}{3}\frac{a_{2\psi}}{a_{3\psi}} + S + T$.
III Find the two complex poles' parameters $\omega_n = \sqrt{\frac{1}{-pa_{3\psi}}}$, $\zeta = \frac{\sqrt{-pa_{3\psi}}}{2}\left(\frac{a_{2\psi}}{a_{3\psi}} + p\right)$.
IV Calculate the new, simpler, transfer function (17) where $\bar{b}_{1\psi} = b_{1\psi} + \frac{1}{p}$, $\bar{a}_{1\psi} = \frac{2\zeta}{\omega_n}$, $\bar{a}_{2\psi} = \frac{1}{\omega_n^2}$.

$$\frac{\psi}{\psi_{ref}} \approx \frac{\bar{b}_{1\psi} s + 1}{\bar{a}_{2\psi} s^2 + \bar{a}_{1\psi} s + 1} \tag{17}$$

2) Line following controller: According to Fig. 4, open loop transfer function is given with $\frac{d}{\psi_{ref}} = -\frac{u_r}{s}\frac{\psi}{\psi_{ref}}$. where $\frac{\psi}{\psi_{ref}}$ is described with (17). The line following controller is than given with

$$\psi_{ref} = -K_\psi \psi - K_r r - K_d d + K_{Id} \int_0^t (d_{ref} - d)\, dt \tag{18}$$

which yields the closed loop transfer function (19) with $a_0 = \frac{u_r K_{Id}}{\bar{a}_{2\psi} + \bar{b}_{1\psi} K_r}$, $a_1 = \frac{u_r K_d + \bar{b}_{1\psi} K_{Id} u_r}{\bar{a}_{2\psi} + \bar{b}_{1\psi} K_r}$, $a_2 = \frac{1 + K_\psi + \bar{b}_{1\psi} K_d u_r}{\bar{a}_{2\psi} + \bar{b}_{1\psi} K_r}$ and $a_3 = \frac{\bar{a}_{1\psi} + K_r + \bar{b}_{1\psi} K_\psi}{\bar{a}_{2\psi} + \bar{b}_{1\psi} K_r}$.

$$\frac{d}{d_{ref}} = \frac{\left(\bar{b}_{1\psi} s + 1\right) a_0}{s^4 + a_3 s^3 + a_2 s^2 + a_1 s + a_0} \tag{19}$$

From here, the controller parameter vector $\Theta_K = \begin{bmatrix} K_r & K_\psi & K_d & K_{Id} \end{bmatrix}$ can be calculated by solving the matrix equation (20).

$$\begin{bmatrix} 1 - a_3\bar{b}_{1\psi} & \bar{b}_{1\psi} & 0 & 0 \\ -a_2\bar{b}_{1\psi} & 1 & \bar{b}_{1\psi}u_r & 0 \\ -a_1\bar{b}_{1\psi} & 0 & u_r & u_r b_{1\psi} \\ -a_0\bar{b}_{1\psi} & 0 & 0 & u_r \end{bmatrix} \Theta_K = \begin{bmatrix} a_3\bar{a}_{2\psi} - \bar{a}_{1\psi} \\ a_2\bar{a}_{2\psi} \\ a_1\bar{a}_{2\psi} \\ a_0\bar{a}_{2\psi} \end{bmatrix} \tag{20}$$

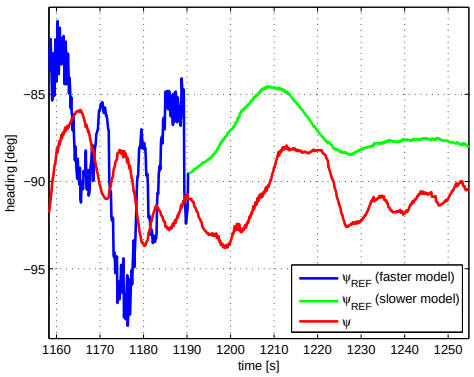

Fig. 5. Rudder activity for two different model functions.

3) Algorithm: The algorithm for designing line following controllers according to Method 2 is as follows.

I Perform two self-oscillation experiments on a closed loop steering system (9) and determine magnitudes X_{m1}, X_{m2} and frequencies ω_1, ω_2 of self-oscillations.
II Calculate $a_{3\psi}$, $a_{2\psi}$, $a_{1\psi}$ and $b_{1\psi}$ using (10).
III Use the Algorithm for simplification of heading closed loop transfer function to calculate $\bar{a}_{2\psi}$, $\bar{a}_{1\psi}$ and $\bar{b}_{1\psi}$.
IV Define desired line following closed loop dynamics (a_4, a_3, a_2 and a_1).
V Calculate line following controller parameters using (20).
VI Implement line following controller using algorithm (18).

IV. Experimental Results

The following section will give experimental results for line following responses. All controllers are tuned using the IS-O method. The tuning of line following controllers using Method 2 was tested with two different closed loop structures: Case 1 is achieved by a P-D controller and Case 2 by a I-PD heading controller. These experiments were performed to demonstrate that the proposed methodology works for various inner loop control structures.

A. Choosing the Model Transfer Function

A model transfer function used in controller design for both cases has to be chosen appropriately. Given the fact that during transient response rudder is almost always saturated (in order to achieve fast dynamics), the criterion for choosing the model transfer function is rudder activity. It is required that rudder activity in steady-state is low in order to minimize energy consumption and mechanical stress. Fig. 5 clearly demonstrates this issue. First $30s$ of the response is with model function in Bessel form with characteristic frequency $\omega_c = 0.5s^{-1}$ ("faster" model). The following part of the response is with model Bessel function with $\omega_c = 0.211s^{-1}$ ("slower model"). Since the model function describes only input-output behavior of the closed loop, internal signals have to be checked a posteriori.

B. IS-O for Methods 1 & 2

The relay parameters for both methods can be found in Table II. For Method 1, relay output was commanded rudder angle δ, while for Method 2 it was commanded heading ψ_{ref}. Experiments for Methods 1 & 2 are shown in Fig. 6(a) and Fig. 6(b), respectively (Case 2 is shown for Method 2). In both cases, duration of the experiment is short and last about 5 oscillations per experiment. The relay parameters for Method 2 were chosen in such a way that the rudder during the experiments never saturates. This is very important because only in that case true inner loop dynamics can be identified.

TABLE II
Relay parameters for cases 1 & 2.

Method	Case	IS-O Experiment #1	IS-O Experiment #2
1		$C = 25°$, $x_a = 10°$	
2	1	$C = 20°$, $x_a = 5°$	$C = 15°$, $x_a = 5°$
2	2	$C = 10°$, $x_a = 5°$	$C = 30°$, $x_a = 10°$

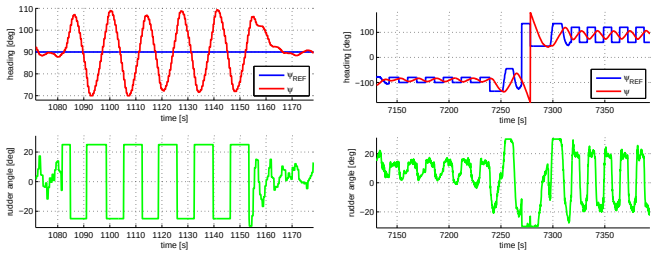

(a) (b)

Fig. 6. IS-O results for (a) Method 1 and (b) Method 2 (Case 2)

C. Results for Method 1

The path is shown in Fig. 7(a) and responses during the path in Fig. 7(b). If controller output is not saturated, the vehicle might start circling. This is why the controller output is saturated so that the approach angle to the line is $30°$.

D. Results for Method 2, Cases 1 & 2

The paths for cases 1 and 2 are shown in Fig. 8(a) and Fig. 9(a), respectively. Corresponding responses are shown in Fig. 8(b) and Fig. 9(b), respectively. In both cases, the approach angle to the line (controller output) is saturated to $30°$. The results show that rudder activity in steady state is sufficiently low and that line following is performed without error. This proves that design procedure is valid and can be used regardless of the inner loop structure.

V. Conclusion

The paper presents the use of IS-O method applied to designing line following controllers. The proposed controllers were applied to autonomous catamaran Charlie. Two approaches are presented. The first, where controller outputs reference yaw rate, is used when low level controllers can be tuned. The second, where output is reference heading, is used when heading controller is already tuned. For this approach results are given for two cases demonstrating how the proposed methodology does not depend on the heading controller structure. Both approaches have proved to be simple and feasible in field conditions. In addition to that, controllers

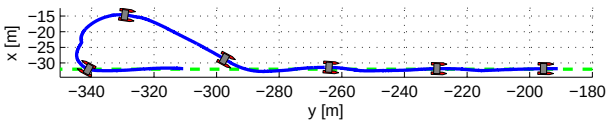

(a)

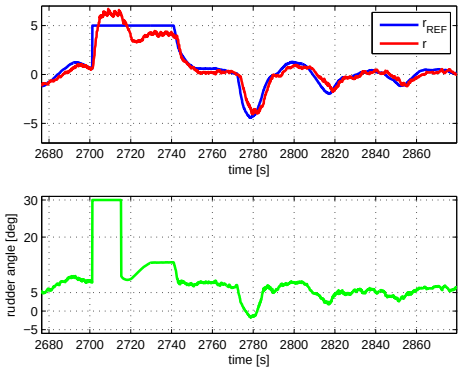

(b)

Fig. 7. Method 1: (a) U-turn and line following, (b) responses

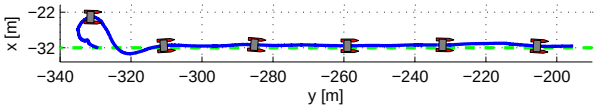

(a)

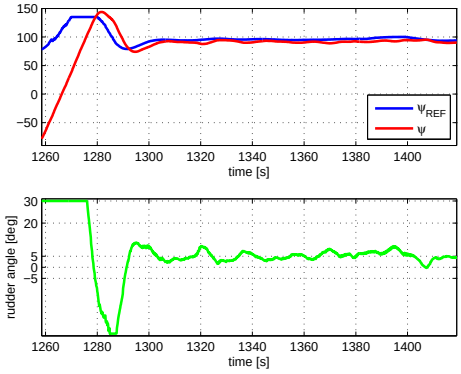

(b)

Fig. 8. Method 2, Case 1: (a) U-turn and line following, (b) responses

demonstrated satisfactory performance: low rudder activity and small steady-state error.

ACKNOWLEDGMENT

The authors would like to thank Giorgio Bruzzone and Edoardo Spirandelli for their fundamental support in the development and operation of the Charlie USV, and *Associazione Prà Viva* for their kind help in allowing the experiments to take place on their ground.

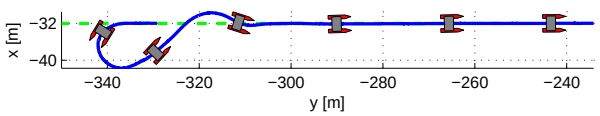

(a)

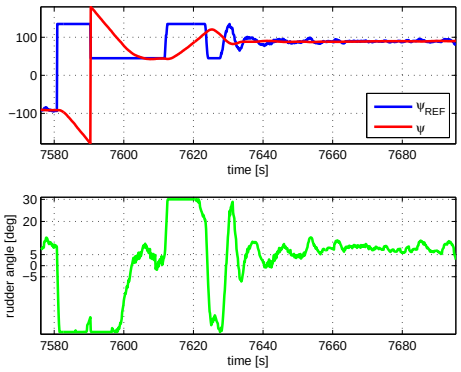

(b)

Fig. 9. Method 2, Case 2: (a) U-turn and line following, (b) responses

REFERENCES

[1] M. Caccia, G. Bruzzone, and R. Bono, "Modelling and identification of the charlie2005 asc," *Proc. of IEEE 14th Mediterranean Conference on Control and Automation*, 2006.

[2] P. Ridao, A. Tiano, A. El-Fakdi, M. Carreras, and A. Zirilli, "On the identification of non-linear models of unmanned underwater vehicles," *Control Engineering Practice*, vol. 12, pp. 1483–1499, 2004.

[3] M. Stipanov, N. Miskovic, Z. Vukic, and M. Barisic, "Rov autonomization - yaw identification and automarine module architecture," *Proc. of the CAMS'07 Conference*, 2007.

[4] N. Miskovic, Z. Vukic, and M. Barisic, "Identification of coupled mathematical models for underwater vehicles," *Proc. of the OCEANS'07 Conference*, 2007.

[5] Z. Vukic, L. Kuljaca, D. Donlagic, and S. Tesnjak, *Nonlinear Control Systems*. New York: Marcel Dekker, 2003.

[6] N. Miskovic, Z. Vukic, and M. Barisic, *Identification of Underwater Vehicles for the Purpose of Autopilot Tuning - Intelligent Underwater Vehicles*. Vienna: InTech Education and Publishing, 2009.

[7] M. Caccia, R. Bono, G. Bruzzone, G. Bruzzone, E. Spirandelli, G. Veruggio, A. Stortini, and G. Capodaglio, "Sampling sea surface with sesamo," *IEEE Robotics and Automation Magazine*, vol. 12(3), pp. 95–105, 2005.

[8] K. J. Åstrom and Hagglund, "Automatic tuning of simple regulators with specifications on phase and amplitude margins," *Proc. of the NGCUV'08 Conference*, vol. 20, p. 645, 1984.

[9] N. Miskovic, Z. Vukic, M. Barisic, and B. Tovornik, "Autotuning autopilots for micro-rovs," *Proc. of the 14th Mediterranean Conference on Control and Applications*, 2006.

[10] N. Miskovic, Z. Vukic, M. Barisic, and P. Soucacos, "Auv identification by use of self-oscillations," *Proc. of the CAMS'07 Conference*, 2007.

[11] M. Bibuli, G. Bruzzone, M. Caccia, N. Miskovic, and Z. Vukic, "Self-oscillation based identification and heading control of unmanned surface vehicles," *Proc. of the RAAD'08 Conference*, 2008.

[12] N. Miskovic, Z. Vukic, and M. Barisic, "Transfer function identification by using self-oscillations," *Proc. of the 15th Mediterranean Conference on Control and Applications*, 2007.

[13] Z. Vukic and L. Kuljaca, *Automatic Control - Analysis of Linear Systems (in Croatian)*. Zagreb: Kigen, 2005.

[14] N. Miskovic, Z. Vukic, and E. Omerdic, "Control of uuvs based upon mathematical models obtained from self-ocillations experiments," *Proc. of the NGCUV'08 Conference*, 2008.